CHEMISTRY OF MATERIALS

Article

pubs.acs.org/cm

Odd−Even Structural Sensitivity on Dynamics in Network-Forming Ionic Liquids

Ke Yang,[†,‡] Zhikun Cai,[§] Madhusudan Tyagi,[⊥,¶] Mikhail Feygenson,[▽] Joerg C. Neuefeind,[▽] Jeffrey S. Moore,*[,†,‡,∥] and Yang Zhang*[,†,‡,§]

[†]Beckman Institute for Advanced Science and Technology, [‡]Department of Materials Science and Engineering, [§]Department of Nuclear, Plasma, and Radiological Engineering, and [∥]Department of Chemistry, University of Illinois at Urbana−Champaign, Urbana, Illinois 61801, United States

[⊥]NIST Center for Neutron Research, National Institute for Standards and Technology, Gaithersburg, Maryland 20899, United States

[▽]Chemical and Engineering Materials Division, Oak Ridge National Laboratory, Oak Ridge, Tennessee 37831, United States

[¶]Department of Materials Science and Engineering, University of Maryland, College Park, MD 20742, United States

Supporting Information

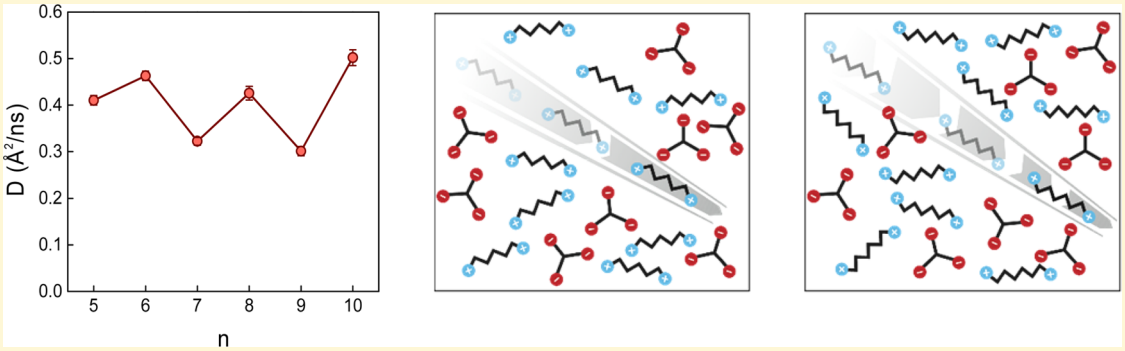

ABSTRACT: As a compelling case of sensitive structure−property relationship, an odd−even effect refers to the alternating trend of physical or chemical properties on odd/even number of repeating structural units. In crystalline or semicrystalline materials, such odd−even effects emerge as manifestations of differences in the periodic packing patterns of molecules. Therefore, due to the lack of long-range order, such an odd−even phenomenon is not expected for dynamic properties in amorphous state. Herein, we report the discovery of a remarkable odd−even effect of dynamical properties in the liquid phase. In a class of glass-forming diammonium citrate ionic liquids, using incoherent quasi-elastic neutron scattering measurements, we measured the dynamical properties including diffusion coefficient and rotational relaxation time. These directly measured molecular dynamics showed pronounced alternating trends with increased number of methylene ($-CH_2-$) groups in the backbone. Meanwhile, the structure factor $S(Q)$ showed no long-range periodic packing of molecules, while the pair distribution function $G(r)$ revealed subtle differences in the local molecular morphology. The observed dynamical odd−even phenomenon in liquids showed that profound dynamical changes originate from subtle local structural differences.

INTRODUCTION

Bridging molecular structure and macroscopic phenomena has been an ultimate dream of chemists since the inception of modern chemistry.[1−6] Under some rare circumstances, material properties show surprising sensitivity with respect to their electronic, atomic, or molecular structures. For instance, the chemical reactivity between carbon nanotube and diazonium salts is highly sensitive to the electronic structure of carbon nanotube;[7] the activation energy of methane CH bond activation is strongly sensitive to the surface atom structure;[8] and polyisocyanates with stereospecifically deuterated side chains manifest completely opposite helical conformation from slight chiral differences in monomer and precursors.[9] The fact that minor structure changes result in significant differences in material properties is intriguing for fundamental research and crucial for practical applications.

As an exemplification of structure−property relationships, odd−even effects reflect sensitivity of minor structural changes to properties within homologous materials. This sensitivity exists at different length scales and involves different types of interactions.[10−12] Nevertheless, all known odd−even effects are related to packing, where the significant alternation of macroscopic properties is manifested from long-range periodic packing of molecules. Indeed, the classic example, taught in most organic chemistry textbooks, is probably *n*-alkanes, where

Received: April 9, 2016
Revised: April 12, 2016
Published: April 13, 2016

DOI: 10.1021/acs.chemmater.6b01429
Chem. Mater. 2016, 28, 3227−3233

the melting points have an odd−even effect with chain length. Its molecular-level explanation is that even-numbered *n*-alkanes have more optimal intermolecular contacts than odd-numbered *n*-alkanes, leading to less dense lattice packing. Consequently, odd-numbered *n*-alkanes have lower density, lower melting point, and smaller fusion enthalpy than even-numbered neighbors.[13] Similarly, the odd−even trend on thermodynamic properties of the solids can be justified insofar by packing effects. On the other hand, liquid-phase properties of these systems only show monotonic dependencies on the repeating structure units because of the absence of periodic packing; for instance, the boiling point of *n*-alkane does not show an odd−even variation. Near melting point, there are rare instances where accurate measurements revealed slight odd−even effect for properties in liquid state such as volume/density.[14]

Despite the existence of odd−even effects in various systems, an odd−even effect of dynamic properties was rarely reported in literature. An early case is the odd−even effect on viscoelastic properties in nematic liquid crystals. Rotational viscosity of these liquid crystals exhibits an alternation trend with alkyl chain length.[15−17] More recent molecular dynamics (MD) simulation produced slight odd−even effects on rotational diffusion coefficients.[18] Another case is that, in several alkylimidazolium- and pyrrolidinium-based ionic liquids, the viscosity also exhibits subtle odd−even trends with increasing alkyl chain length.[19−21] MD simulation predicted that the same trend goes with ion diffusion coefficient and electrical conductivity in these ionic liquids.[21,22] Santos and co-workers[23−26] and Dupont and co-workers[27,28] provided nano-structuration evidence in liquid phase regarding the structure−property relationship in imidazolium-based ionic liquid including dissociation energies, volatility, and surface tension. However, in both cases, the structural sensitivity of dynamic-related properties such as viscosity and vapor pressure is rather weak. In addition, the experimental measurement of dynamic properties at the molecular level, such as diffusion coefficient, is still lacking.

Herein, we present the discovery of a dynamical odd−even effect in liquid state. We prepared a homologue of glass-forming ionic liquids by coupling stoichiometric diammonium alkyl cations and citrate anions. To study the odd−even effect with fine spatial and temporal resolution, we employed wide-angle neutron and synchrotron diffraction and quasi-elastic neutron scattering. We measured network-forming ionic liquid (NIL) microstructure by X-ray powder diffraction and local structure by neutron and X-ray pair distribution function (PDF) analysis. Both results suggested very slight alternating trend in the local structures of the liquids. We found that the mean squared displacement exhibited an odd−even effect as a function of alkyl backbone length in the cation. The incoherent quasi-elastic neutron scattering measurements revealed significant odd−even effects in dynamic properties such as diffusion coefficient, residence time, and rotational relaxation time. The understanding of such sensitivity of dynamic properties over structures will motivate more fundamental studies on structure−property relationships for molecular viscous flow. We also expect this work to be helpful for technological applications requiring novel materials with structural sensitivity.

RESULTS AND DISCUSSION

All NILs under investigation were synthesized according to a previously reported procedure.[29−31] For brevity, these ionic liquids were named as "NIL $n - m$", where n is the number of methylene units in alkyl backbone and m is the number of methylene/methyl units in side chains. We have chosen this glass-forming liquid over common ionic liquids because the structural difference between glass and liquid state is minimal. For our work, we would like to demonstrate that considerable differences in dynamics could result from slight differences in structure. With excessive structural frustration by alkyl side chains in the cation, the ionic network refused to crystallize upon cooling. Both n and m determined the NIL glass transition temperature as a result of competition between electrostatic and van der Waals forces.

Microstructure analysis of NILs revealed a monotonic trend of major peak position as a function of cation backbone repeating units n. Measured structure factors $S(Q)$ of a series of NILs with n from 3 to 10 showed similar patterns. We observed three major peaks in the measured Q range (Figure 1a). The

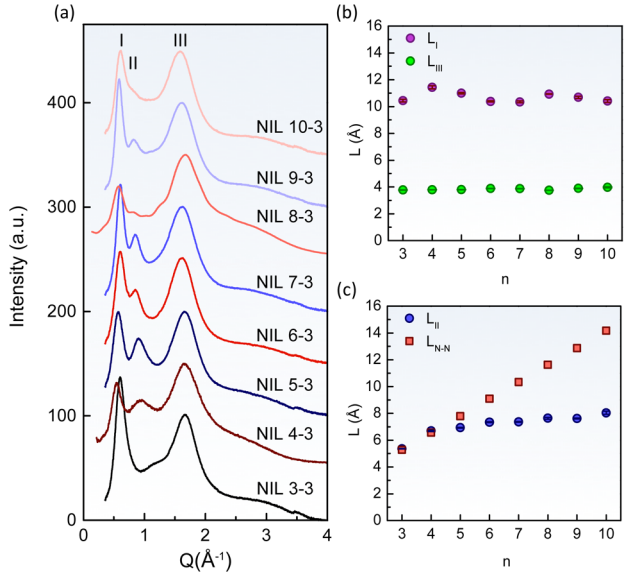

Figure 1. (a) X-ray diffraction (XRD) patterns of a series of NILs (n = 3−10, m = 3). All samples showed similar XRD features with three major peaks in the measured Q range. (b) Extracted corresponding length scale L for peak I and III as a function of n; both L_I and L_{III} are rather independent of n. (c) Extracted corresponding length scale L for peak II and theoretical fully extended backbone length L_{N-N} as a function of n; L_{II} varies monotonically with n and does not show an alternating trend.

positions of peaks I and III are rather independent of n, while that of peak II shifted to lower Q direction with larger n. We estimated the corresponding spatial correlation length as $L = 2\pi/Q_{max}$ (Figure 1b). L_I and L_{III} did not show any obvious dependence on n. For comparison, we plotted the fully extended N−N distance in the cation of all-trans configuration together with L_{II}. For n = 3 and 4, L_{II} was in accordance with L_{N-N} in the cation. However, with longer backbone chain length (n > 4), L_{II} varied almost linearly with backbone alkyl chain length, and it deviated from the fully extended N−N distance. It has been reported that L_{II} correlates with the intracation tail−tail correlation based on partial structure factor attribution.[22,32,33] The microstructural analysis provided by powder XRD showed that the packing of molecules in these NILs does not show an alternating trend with backbone repeating units n.

DOI: 10.1021/acs.chemmater.6b01429
Chem. Mater. 2016, 28, 3227−3233

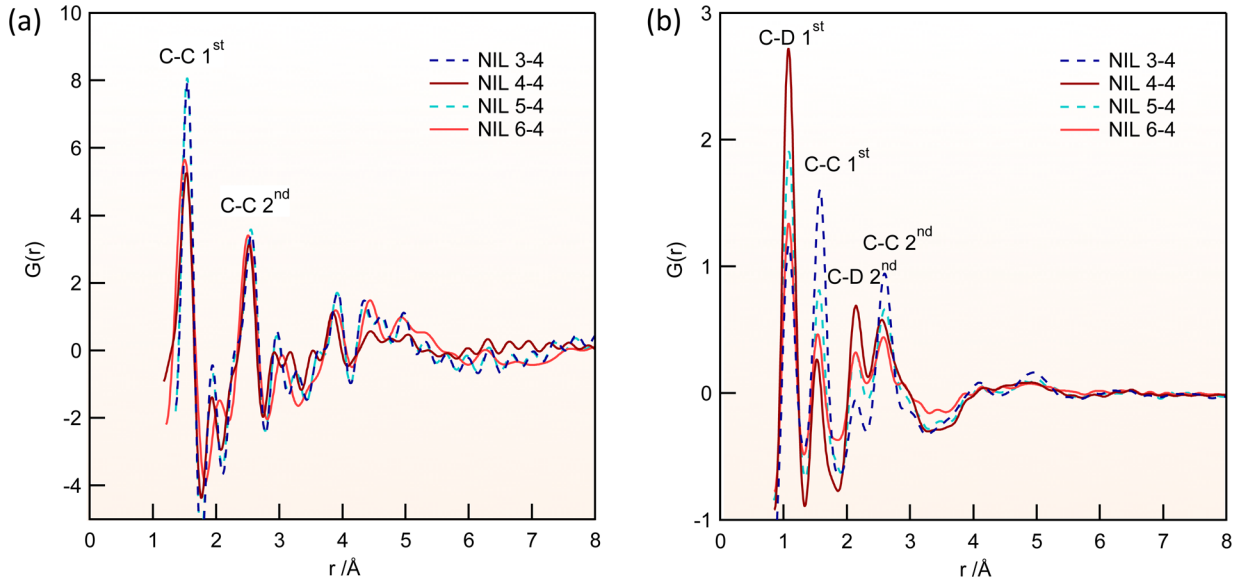

Figure 2. (a) X-ray pair distribution function (XPDF) of normal protonated sample NIL $n - 4$ at 300 K. (b) Neutron pair distribution function (NPDF) of deuterated sample NIL $n - 4$ at 300 K. In both NPDF and XPDF, the number of C−C first neighbors of odd-NILs was larger than for even-NILs; in NPDF, the number of C−D first neighbors of even-NILs was larger than for odd-NILs. These odd−even local structural differences are hard to identify beyond second nearest neighbors of C−C and C−D.

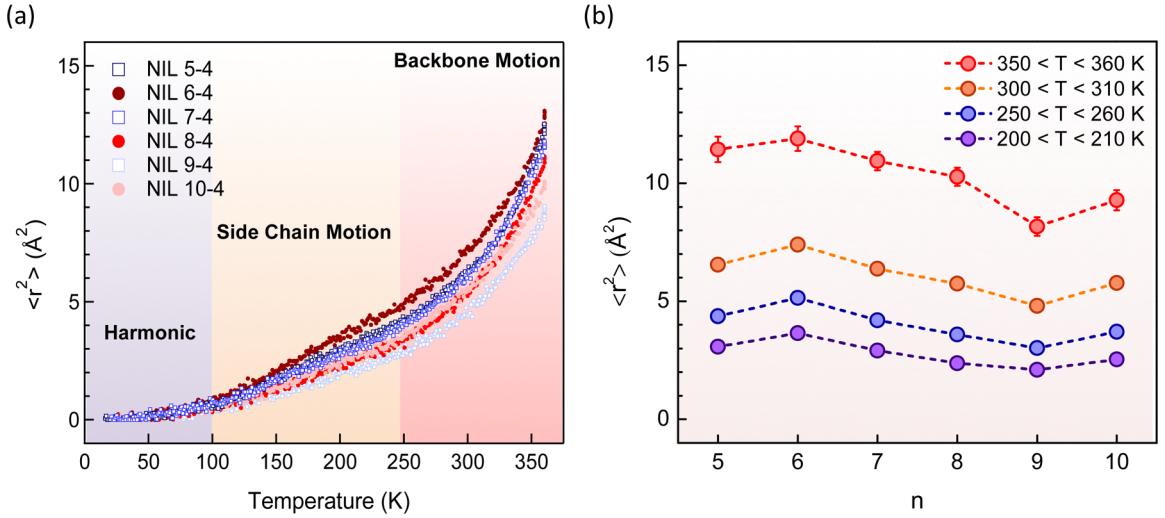

Figure 3. (a) Temperature dependence of mean squared displacement (MSD) of NIL series $n - 4$ (n = 5−10). (b) Average MSD of different temperature ranges as a function of backbone repeating units, showing clear odd−even alternation. The alternating trend that even-NILs have larger MSD values than odd-NILs becomes clearer at higher temperature. Error bars throughout the text represent one standard deviations.

After ruling out the alternating trend in NIL microstructures, we decided to check whether the local structures of NILs could reveal any alternating trend. Pair distribution function (PDF) analysis using both synchrotron X-rays and neutrons gave local (r < 10 Å) structural information on atoms in NILs. Such local structural information is dominated by intramolecular atomic correlations, although cross-correlations between molecules also contribute to the scattering signal. We collected PDF data in the liquid state at 300 K (Figure 2). The local structures of NILs and their corresponding glass states were almost identical. The PDFs were very close with only slight difference on some peak heights, such as a decreased intensity of the first peak at 300 K at 1.07 Å. For X-ray pair distribution function (XPDF) measurements, we used normal hydrogenated samples. Due to the negligible X-ray cross sections of hydrogen atoms, the XPDF mainly revealed C−C correlations with the prominent first two peaks at 1.55 and 2.7 Å. Scattering from the two N atoms in the cation is weak compared to the majority C atoms. The number of nearest C−C neighbors (1.55 Å) was found to be larger for odd-NILs than for even-NILs. However, such odd−even local structural differences can no longer be identified beyond the second nearest neighbor of C−C. In order to reveal the hydrogen ordering, we synthesized deuterated samples for neutron pair distribution function (NPDF) measurements. In addition to the C−C correlations, similarly to what was observed in XPDF, the NPDF further revealed two prominent C−D correlations at 1.07 and 2.1 Å. On the contrary to C−C coordination number, the number of the first (1.07 Å) and second (2.1 Å) C−D neighbors was found to be smaller for odd-NILs than for even-NILs. The alternating trend of C−C and C−D correlations revealed by PDF analysis indicates that a weak odd−even effect of

DOI: 10.1021/acs.chemmater.6b01429
Chem. Mater. 2016, 28, 3227−3233

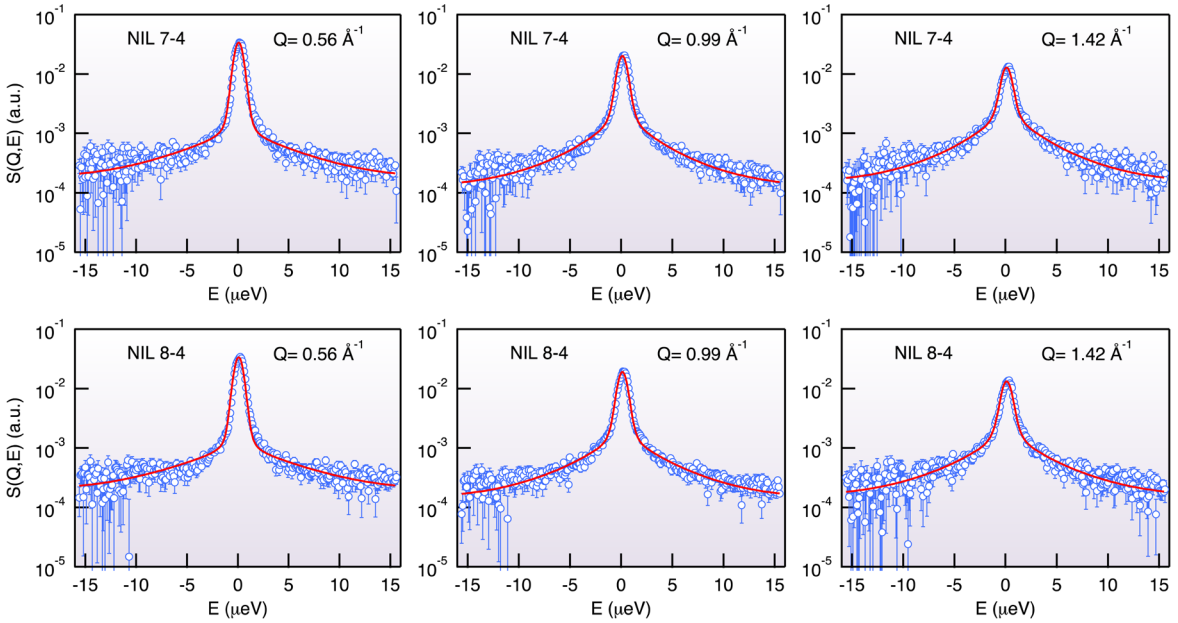

Figure 4. Quasi-elastic neutron scattering (QENS) spectra of samples NIL 7−4 and NIL 8−4 at three representative Q values. Red lines represent fits with the translational random-jump-diffusion and rotational Sears expansion model. The model was able to capture key features in the measured QENS spectra in all Q ranges and fit all data remarkably well.

molecular morphology exists in NILs. It is interesting to note that such local molecular morphology differences are so weak that they do not translate into any long-range odd−even packing of the molecules, as evidenced in the previous XRD data.

We then investigated the molecular-scale dynamics of NILs using incoherent elastic neutron scattering (IENS). We chose the butyl side chain ($m = 4$) series for dynamic study because of the match of their dynamic features to the time window of the back scattering instrument.[34] Due to the exceptionally large incoherent cross section of hydrogen atoms, IENS probes hydrogen motions. As most of the hydrogen atoms are in the cations, the measurement predominantly probed the motions of cations. The measured intensity is proportional to the effective Debye−Waller factor, $\exp[-{}^1/_6\langle r^2\rangle Q^2]$, of the hydrogen atoms in the system, averaged over the nanosecond time resolution window, which directly yields the hydrogen mean squared displacement (MSD). As shown in Figure 3a, measured temperature dependence of the MSD can be divided into three regimes: harmonic motion, side-chain motion, and backbone motion. From 100 to 250 K, the first increase of MSD started to emerge. This increase of MSD is due to rotational motion and confined-segment motion in NILs. It is noticeable that the even-numbered NILs show larger MSD values than neighboring odd-numbered ones in this regime. Above 250 K, backbone motion dominated. The MSDs increased dramatically in this regime due to diffusions of the whole ion. In this regime, larger differences between odd- and even-numbered cations are observed. We plot the average MSDs within four different temperature ranges (10 K for each range) as functions of the backbone repeating units n (Figure 3b). For the two higher-temperature ranges, we observed more obvious odd−even effects on average MSD values than for lower temperatures. Note that this dynamical odd−even effect was observed in liquid states in the absence of any long-range order.

To take a step further, we measured the diffusional dynamics of NILs using quasi-elastic neutron scattering (QENS) at 360 K. The wave-vector transfer Q and energy transfer E dependence of the scattering intensity, basically the double-differential cross section, is described by the Fourier transform of the self-intermediate scattering function:

$$I(Q, E) = N\mathcal{F}\{F_s(Q, t)\} \otimes R(Q, E) \quad (1)$$

where N is the normalization factor, $F_s(Q,t)$ is the self-intermediate scattering function, and $R(Q,E)$ is the Q-dependent energy resolution function. $F_s(Q,t)$ can be further decoupled as the product of the translational correlation function $F_T(Q,t)$ and the rotational correlation function $F_R(Q,t)$ of the hydrogens of the cations:

$$F_s(Q, t) = A(Q)F_T(Q, t)F_R(Q, t) \quad (2)$$

where $A(Q)$ represents the fast motions of atoms outside the time window of the measurements and is fixed at unity because of its coupling with the normalization factor N. $F_T(Q,t)$ represents the contribution from translational diffusion. For a simple liquid, it can be described by the random-jump-diffusion model:

$$F_T(Q, t) = \exp\left(-\frac{t}{\tau_T}\right)$$

$$\frac{1}{\tau_T} = \frac{DQ^2}{1 + DQ^2\tau_0} \quad (3)$$

where D is the translational diffusion coefficient and τ_0 is the residence time between random jumps of particles.[35]

$F_R(Q,t)$ represents the rotational diffusion of a molecule. Its Q and t dependence can be separated by the Sears expansion.[36] Here we terminate the expansion after the first three terms because the higher-order terms are negligible in our experimental Q range. Thus, the expression for $F_R(Q,t)$ is

DOI: 10.1021/acs.chemmater.6b01429
Chem. Mater. 2016, 28, 3227−3233

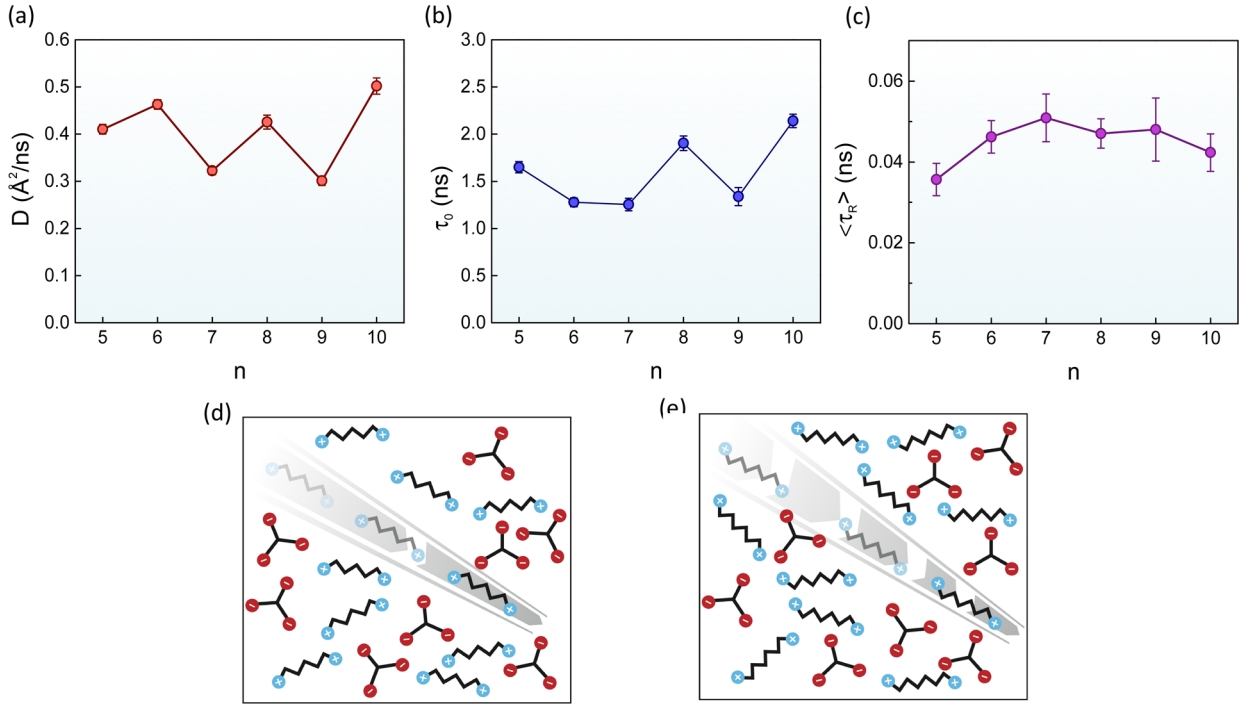

Figure 5. (a) Diffusional coefficient D, (b) random-jump-diffusion residence time τ_0, and (c) rotational relaxation time τ_R as functions of backbone repeating units n. (d, e) Schematic depiction of dynamic odd−even effect of NILs: odd-NILs cations (d) move more slowly than even-NILs (e). Dynamic properties such as translational diffusional coefficient, residence time, and relaxation time showed sensitivity to backbone repeating units n.

$$F_R(Q, t) = j_0^2(Qa) + 3j_1^2(Qa)\exp[-t/3\tau_R] + 5j_2^2(Qa)\exp[-t/\tau_R] \quad (4)$$

Here a stands for radius of rotation, τ_R is relaxation time associated with rotational diffusion, and $j_n(x)$ are the spherical Bessel functions.

Demonstrations of the fittings of QENS spectra of two samples, NIL 7−4 and NIL 8−4, with this model are illustrated in Figure 4. The model was able to capture key features in the measured QENS spectra in all Q ranges and fit all data remarkably well with three parameters: diffusional relaxation time τ_T (which further yields diffusion coefficient D and residence time τ_0), rotational relaxation time τ_R, and rotational radius a.

For translational motion, diffusion coefficient D exhibited great sensitivity to NIL's odd−even structural units. We plotted the line width of translational component $1/\tau_T$ of the spectrum as a function of Q^2 (Figure S3). For all samples, the trend of line width showed an initial linear region with Q whose slope yielded the diffusion coefficient D, and at higher Q values it flattened out to a plateau that defines random-jump-diffusion residence time τ_0. As shown in Figure 5a, translational diffusion coefficient D exhibited a remarkable odd−even trend as a function of backbone repeating units n of the cation. Odd-numbered cations showed significantly smaller diffusion coefficients than neighboring even-numbered ones. This observation was consistent with, yet more striking than, the MSD trend described previously. The largest difference of neighboring odd- and even-numbered NILs was between NIL 9−4 and NIL 10−4. With one additional methylene unit, the diffusion coefficient differed by almost a factor of 2. For residence time τ_0 (Figure 5b), there is also a similar alternation trend (except for the case n = 6, which may be due to uncertainties in measurements and analysis). The general trend was that even-numbered cations showed a longer residence time between jump-diffusion events.

Further analysis of rotational motion also reveals a similar odd−even effect. From the rotational contribution $F_R(Q,t)$, two essential parameters can be extracted: radius of rotation a and rotational relaxation time τ_R. All samples exhibited similar trends of correlation between rotation radius a and wave-vector transfer Q: a decreased in low-Q regime ($Q < 0.75$ Å^{-1}) and flattened out to about 1 Å, which corresponded to the C−H distance (Figure S4b). For all NIL samples, rotational relaxation time τ_R was almost independent of Q, especially in the range $0.56 < Q^2 < 2.81$ Å^{-2} (Figure S4a). Interestingly, the mean rotational relaxation time $\langle\tau_R\rangle$ over the measured the Q range also showed an odd−even trend toward backbone repeating units n (Figure 5c).

Without noticeable packing differences, the diffusion coefficient and residence time of NIL changed significantly with addition of only one methylene group (Figure 5d,e). This extent of structural sensitivity to dynamical properties is surprising given the absence of long-range order in liquid state. Therefore, such an observation challenges the conventional understanding of the odd−even effect in terms of molecular packing. Our results suggest that single molecular morphology, although subtle as shown in the local pair distribution functions, could still result in striking macroscopic dynamic differences. Understanding the principles governing this structure−property relationship is important for design and synthesis of responsive materials. Such molecular structural sensitivity of dynamics is reminiscent of a glass transition process, where the transport properties of molecules change by several orders of magnitude while the differences between intermolecular structures can hardly be appreciated. The dynamical odd−even effect could also provide new insight into molecular viscous flow.

DOI: 10.1021/acs.chemmater.6b01429
Chem. Mater. 2016, 28, 3227−3233

In summary, we discovered a dynamic odd−even effect in liquids. Microstructure analysis by powder XRD showed similar arrangements of molecular ions for homologues of ionic liquids. However, neutron and X-ray PDF analysis reveal that molecular morphology exhibits a weak alternating trend as a function of repeating methylene units. Elastic neutron scattering suggests that the odd−even trend of nanosecond MSD as a function of n is very clear at high temperature. Further QENS measurements conducted in liquid state confirm that odd−even trends exist in diffusion coefficient of translational motion, residence time, and rotational motion. Such great sensitivity of dynamical properties with respect to the repeating methylene units in cations is very intriguing. Studies of this structure−dynamic relationship will further bridge the understanding of molecular structures and properties of liquids.

METHODS

Synthesis of Network-Forming Ionic Liquid Series and Sample Preparation for Neutron Scattering. NILs were synthesized according to a previously reported procedure.[31] These materials were prepared by reacting a dibromoalkane with a trialkylamine. The bromide counteranion was then replaced with hydroxide by use of an anion-exchange column. In situ reaction with citric acid (or other polyacids) gave the desired products and water, followed by drying under vacuum at 323 K for 2 days.

Deuterated NILs were synthesized from deuterated dibromoalkane, trialkylamine, and citric-2,2,4,4-d_4 ccid for neutron PDF experiments. Deuterated reagents were purchased from C/D/N Isotopes Inc. with at least 98 at. % deuterium. All deuterated materials were fully deuterated except citric-2,2,4,4-d_4 acid, which had one hydrogen on the hydroxide group. Identification of a commercial product does not imply recommendation or endorsement by the NIST, nor does it imply that the product is necessarily the best for the stated purpose.

Quasi-elastic Neutron Scattering Experiment. The QENS experiment was carried out on the high-flux backscattering (HFBS) instrument at NIST Center for Neutron Research (NCNR). Thin layers of samples were loaded into cylindrical aluminum containers. Helium glovebox was used in order to avoid moisture and enhance heat conductivity. The sample cans were sealed with indium wires. The sealed sample container was then mounted in a top-loading closed-cycle refrigerator (CCR) with temperature accuracy better than 0.1 K. The nominal incident neutron wavelength was 6.271 Å (2.08 meV in energy). The instrument was first operated in the fixed-window mode, that is, the Doppler drive was stopped. In this mode, only elastically scattered neutrons were detected. The temperature was continuously ramped up from 15 to 363 K with a heating rate of 1 K/min.

After the fixed-window scan, the instrument was operated in dynamic-window mode, where the Doppler drive was operated in such a way to provide an energy transfer range of ±17 μeV, for a wave-vector transfer Q range of 0.25−1.75 Å^{-1}. Energy resolution near the elastic line was about 1 μeV. All quasi-elastic measurements were taken at 360 K, where all samples were in the liquid phase. Vanadium run was used for detector calibration and instrument resolution.

X-ray and Neutron Pair Distribution Function Experiments. The X-ray PDF experiment was conducted at beamline 11-ID-B of the Advanced Proton Source (APS) at Argonne National Laboratory (ANL) with incident X-ray energy of 58.66 keV. Samples were settled inside Kapton capillaries and sealed with epoxy. Samples were aligned in both horizontal and vertical directions within the X-ray beam. Measurements were carried out at room temperature in ambient conditions. The scattering structure factor, with corrections for background scattering, X-ray transmission, and Compton scattering, was obtained from diffraction data by use of the PDFgetX2 software package.[37]

The neutron PDF experiment was conducted at the nanoscale-ordered materials diffractometer (NOMAD) beamline of the Spallation Neutron Source (SNS) at Oak Ridge National Laboratory (ORNL).[38] Deuterated samples were used to reduce incoherent scattering from hydrogen. Samples were sealed inside 3 mm quartz capillaries. The room-temperature measurement took about 0.5 h to obtain high-resolution PDF.

ASSOCIATED CONTENT

Supporting Information

The Supporting Information is available free of charge on the ACS Publications website at DOI: 10.1021/acs.chemmater.6b01429.

Additional text with extended methods description; one scheme showing chemical structure of NIL series; four figures showing temperature dependence of MSD, QENS spectra, and translational and rotational broadening line width as a function of Q^2 (PDF)

AUTHOR INFORMATION

Corresponding Authors

*E-mail jsmoore@illinois.edu (J.S.M.).
*E-mail zhyang@illinois.edu (Y.Z.).

Notes

The authors declare no competing financial interest.

ACKNOWLEDGMENTS

Y.Z. is supported by ACS PRF 55642-DNI6 and by the U.S. Department of Energy, Office of Science, Office of Basic Energy Sciences, Materials Sciences and Engineering Division, under Award DE-SC-0014804. This work utilized facilities supported in part by the National Science Foundation under Agreement DMR-1508249. Part of the research conducted at ORNL's SNS and ANL's APS was sponsored by the Scientific User Facilities Division, Office of Basic Energy Sciences, U.S. Department of Energy.

REFERENCES

(1) Matta, C. F.; Bader, R. F. W. Atoms-in-Molecules Study of the Genetically Encoded Amino Acids. III. Bond and Atomic Properties and Their Correlations with Experiment Including Mutation-Induced Changes in Protein Stability and Genetic Coding. *Proteins: Struct., Funct., Genet.* **2003**, *52*, 360−399.

(2) Shimomura, M.; Sawadaishi, T. Bottom-up Strategy of Materials Fabrication: A New Trend in Nanotechnology of Soft Materials. *Curr. Opin. Colloid Interface Sci.* **2001**, *6*, 11−16.

(3) Lu, W.; Lieber, C. M. Nanoelectronics from the Bottom Up. *Nat. Mater.* **2007**, *6*, 841−850.

(4) Zhang, S. Fabrication of Novel Biomaterials through Molecular Self-Assembly. *Nat. Biotechnol.* **2003**, *21*, 1171−1178.

(5) Katritzky, A. R.; Maran, U.; Lobanov, V. S.; Karelson, M. Structurally Diverse Quantitative Structure-Property Relationship Correlations of Technologically Relevant Physical Properties. *J. Chem. Inf. Comput. Sci.* **2000**, *40*, 1−18.

(6) Jancar, J.; Douglas, J. F.; Starr, F. W.; Kumar, S. K.; Cassagnau, P.; Lesser, A. J.; Sternstein, S. S.; Buehler, M. J. Current Issues in Research on Structure-Property Relationships in Polymer Nanocomposites. *Polymer* **2010**, *51*, 3321−3343.

(7) Strano, M. S.; Dyke, C. A.; Usrey, M. L.; Barone, P. W.; Allen, M. J.; Shan, H.; Kittrell, C.; Hauge, R. H.; Tour, J. M.; Smalley, R. E. Electronic Structure Control of Single-Walled Carbon Nanotube Functionalization. *Science* **2003**, *301*, 1519−1522.

(8) Van Santen, R. A. Complementary Structure Sensitive and Insensitive Catalytic Relationships. *Acc. Chem. Res.* **2009**, *42*, 57−66.

(9) Green, M. M.; Peterson, N. C.; Sato, T.; Teramoto, A.; Cook, R.; Lifson, S. A Helical Polymer with a Cooperative Response to Chiral Information. *Science* **1995**, *268*, 1860−1866.

DOI: 10.1021/acs.chemmater.6b01429
Chem. Mater. 2016, 28, 3227−3233

(10) Häkkinen, H.; Landman, U. Gold Clusters (Au_N, $2 \leq N \leq 10$) and Their Anions. *Phys. Rev. B: Condens. Matter Mater. Phys.* **2000**, *62*, R2287−R2290.
(11) Zhao, J.; Yang, J.; Hou, J. Theoretical Study of Small Two-Dimensional Gold Clusters. *Phys. Rev. B: Condens. Matter Mater. Phys.* **2003**, *67*, No. 085404.
(12) Tao, F.; Bernasek, S. L. Understanding Odd-Even Effects in Organic Self-Assembled Monolayers. *Chem. Rev.* **2007**, *107*, 1408−1453.
(13) Boese, R.; Weiss, H.; Blaser, D. The Melting Point Alternation in the Short-Chain N-Alkanes: Single-Crystal X-Ray Analyses of Propane at 30 K and of N-Butane to N-Nonane at 90 K. *Angew. Chem., Int. Ed.* **1999**, *38*, 988−992.
(14) Adamová, G.; Canongia Lopes, J. N.; Rebelo, L. P. N.; Santos, L. M. N. B.; Seddon, K. R.; Shimizu, K. The Alternation Effect in Ionic Liquid Homologous Series. *Phys. Chem. Chem. Phys.* **2014**, *16*, 4033−4038.
(15) Chen, F.-L.; Jamieson, A. M. Odd-Even Effect in the Viscoelastic Properties of Main-Chain Liquid Crystal Polymer-Low Molar Mass Nematogen Mixtures. *Macromolecules* **1993**, *26*, 6576−6582.
(16) Buchecker, R.; Schadt, M. Synthesis, Physical Properties and Structural Relationships of New, End-Chain Substituted Nematic Liquid Crystals. *Mol. Cryst. Liq. Cryst.* **1987**, *149*, 359−373.
(17) Bock, F.-J.; Kneppe, H.; Schneider, F. Rotational Viscosity of Nematic Liquid Crystals and Their Shear Viscosity under Flow Alignment. *Liq. Cryst.* **1986**, *1*, 239−251.
(18) Capar, M.; Cebe, E. Molecular Dynamic Study of the Odd-Even Effect in Some 4-N-Alkyl-4′-cyanobiphenyls. *Phys. Rev. E* **2006**, *73*, No. 061711.
(19) Rocha, M. A. A.; Neves, C. M. S. S.; Freire, M. G.; Russina, O.; Triolo, A.; Coutinho, J. A. P. C.; Santos, L. M. N. B. F. Alkylimidazolium Based Ionic Liquids: Impact of Cation Symmetry on Their Nanoscale Structural Organization. *J. Phys. Chem. B* **2013**, *117*, 10889−10897.
(20) Martins, M. A. R.; Neves, C. M. S. S.; Kurnia, K. A.; Carvalho, P. J.; Rocha, M. A. A.; Santos, L. M. N. B. F.; Pinho, S. P.; Freire, M. G. Densities, Viscosities and Derived Thermophysical Properties of Water-Saturated Imidazolium-Based Ionic Liquids. *Fluid Phase Equilib.* **2016**, *407*, 188−196.
(21) Leys, J.; Wübbenhorst, M.; Preethy Menon, C.; Rajesh, R.; Thoen, J.; Glorieux, C.; Nockemann, P.; Thijs, B.; Binnemans, K.; Longuemart, S. Temperature Dependence of the Electrical Conductivity of Imidazolium Ionic Liquids. *J. Chem. Phys.* **2008**, *128*, No. 064509.
(22) Zheng, W.; Mohammed, A.; Hines, L. G.; Xiao, D.; Martinez, O. J.; Bartsch, R. A.; Simon, S. L.; Russina, O.; Triolo, A.; Quitevis, E. L. Effect of Cation Symmetry on the Morphology and Physicochemical Properties of Imidazolium Ionic Liquids. *J. Phys. Chem. B* **2011**, *115*, 6572−6584.
(23) Rocha, M. A. A.; Coutinho, J. A. P.; Santos, L. M. N. B. F. Evidence of Nanostructuration from the Heat Capacities of the 1,3-Dialkylimidazolium Bis(trifluoromethylsulfonyl)imide Ionic Liquid Series. *J. Chem. Phys.* **2013**, *139*, No. 104502.
(24) Vilas, M.; Rocha, M. A. A.; Fernandes, A. M.; Tojo, E.; Santos, L. M. N. B. F. Novel 2-Alkyl-1-Ethylpyridinium Ionic Liquids: Synthesis, Dissociation Energies and Volatility. *Phys. Chem. Chem. Phys.* **2015**, *17*, 2560−2572.
(25) Almeida, H. F. D.; Freire, M. G.; Fernandes, A. M.; Lopes-da-Silva, J. A.; Morgado, P.; Shimizu, K.; Filipe, E. J. M.; Canongia Lopes, J. N.; Santos, L. M. N. B. F.; Coutinho, J. A. P. Cation Alkyl Side Chain Length and Symmetry Effects on the Surface Tension of Ionic Liquids. *Langmuir* **2014**, *30*, 6408−6418.
(26) Rocha, M. A. A.; Lima, C. F. R. A. C.; Gomes, L. R.; Schröder, B.; Coutinho, J. A. P.; Marrucho, I. M.; Esperança, J. M. S. S.; Rebelo, L. P. N.; Shimizu, K.; Lopes, J. N. C.; et al. High-Accuracy Vapor Pressure Data of the Extended [C nC 1im][Ntf 2] Ionic Liquid Series: Trend Changes and Structural Shifts. *J. Phys. Chem. B* **2011**, *115*, 10919−10926.
(27) Dupont, J. On the Solid, Liquid and Solution Structural Organization of Imidazolium Ionic Liquids. *J. Braz. Chem. Soc.* **2004**, *15*, 341−350.
(28) Consorti, C. S.; Suarez, P. A. Z.; De Souza, R. F.; Burrow, R. A.; Farrar, D. H.; Lough, A. J.; Loh, W.; da Silva, L. H. M.; Dupont, J. Identification of 1,3-dialkylimidazoIium Salt Supramolecular Aggregates in Solution. *J. Phys. Chem. B* **2005**, *109*, 4341−4349.
(29) Wathier, M.; Grinstaff, M. W. Synthesis and Properties of Supramolecular Ionic Networks. *J. Am. Chem. Soc.* **2008**, *130*, 9648−9649.
(30) Aboudzadeh, M. A.; Muñoz, M. E.; Santamaría, A.; Fernández-Berridi, M. J.; Irusta, L.; Mecerreyes, D. Synthesis and Rheological Behavior of Supramolecular Ionic Networks Based on Citric Acid and Aliphatic Diamines. *Macromolecules* **2012**, *45*, 7599−7606.
(31) Yang, K.; Tyagi, M.; Moore, J. S.; Zhang, Y. Odd-Even Glass Transition Temperatures in Network-Forming Ionic Glass Homologue. *J. Am. Chem. Soc.* **2014**, *136*, 1268−1271.
(32) Song, X.; Hamano, H.; Minofar, B.; Kanzaki, R.; Fujii, K.; Kameda, Y.; Kohara, S.; Watanabe, M.; Ishiguro, S.; Umebayashi, Y. Structural Heterogeneity and Unique Distorted Hydrogen Bonding in Primary Ammonium Nitrate Ionic Liquids Studied by High-Energy X-Ray Diffraction Experiments and MD Simulations. *J. Phys. Chem. B* **2012**, *116*, 2801−2813.
(33) Hettige, J. J.; Araque, J. C.; Margulis, C. J. Bicontinuity and Multiple Length Scale Ordering in Triphilic Hydrogen-Bonding Ionic Liquids. *J. Phys. Chem. B* **2014**, *118*, 12706−12716.
(34) Meyer, A.; Dimeo, R. M.; Gehring, P. M.; Neumann, D. A. The High-Flux Backscattering Spectrometer at the NIST Center for Neutron Research. *Rev. Sci. Instrum.* **2003**, *74*, 2759−2777.
(35) Singwi, K. S.; Sjölander, A. Diffusive Motions in Water and Cold Neutron Scattering. *Phys. Rev.* **1960**, *119*, 863−871.
(36) Sears, V. F. Cold Neutron Scattering By Molecular Liquids: III. Methane. *Can. J. Phys.* **1967**, *45*, 237−254.
(37) Qiu, X.; Thompson, J. W.; Billinge, S. J. L. PDFgetX2: A GUI-Driven Program to Obtain the Pair Distribution Function from X-Ray Powder Diffraction Data. *J. Appl. Crystallogr.* **2004**, *37*, 678.
(38) Neuefeind, J.; Feygenson, M.; Carruth, J.; Hoffmann, R.; Chipley, K. K. The Nanoscale Ordered Materials Diffractometer NOMAD at the Spallation Neutron Source SNS. *Nucl. Instrum. Methods Phys. Res., Sect. B* **2012**, *287*, 68−75.

DOI: 10.1021/acs.chemmater.6b01429
Chem. Mater. 2016, 28, 3227−3233